analytical chemistry

Article

pubs.acs.org/ac

Extracting Kinetics from Affinity Capillary Electrophoresis (ACE) Data: A New Blade for the Old Tool

Mirzo Kanoatov, Leonid T. Cherney, and Sergey N. Krylov*

Department of Chemistry and Centre for Research on Biomolecular Interactions, York University, Toronto, Ontario M3J 1P3, Canada

Supporting Information

ABSTRACT: We describe a mathematical approach that enables extraction of *kinetic rate constants* from thousands of studies conducted over the past two decades with affinity capillary electrophoresis (ACE). Previously, ACE has been used almost exclusively for obtaining *equilibrium constants* of intermolecular interactions. In this article, we prove that there exists an analytical solution of partial differential equations describing mass transfer in ACE. By using an in silico study, we demonstrate that the solution is applicable to experimental conditions that are typically used in ACE and found in most historical ACE experiments. The solution was validated by extracting rate constants from previously published ACE data and closely matching independently obtained results. Lastly, it was used to obtain previously unknown rate constants from historical ACE data. The new mathematical approach expands the applicability of ACE to a wider range of biomolecular interactions and enables both prospective and retrospective data analysis. The obtained kinetic information will be of significant practical value to the fields of pharmacology and molecular biology.

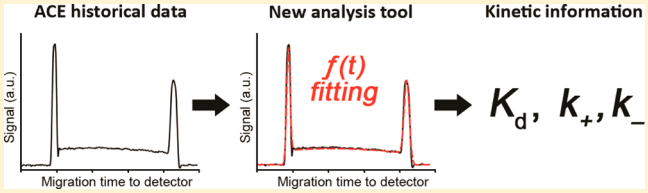

Development of new data-analysis strategies can improve the performance of existing analytical methods. For example, development of the "second derivative" approach for analysis of data for quantitative polymerase chain reaction has significantly increased the precision and accuracy of the method.[1] More interesting, however, is the development of data-analysis strategies that can extract previously inaccessible information from both new and old data. In this article, we introduce a simple mathematical approach which allows deconvolution of kinetic rate constants from data produced by affinity capillary electrophoresis (ACE). ACE is a popular method for determining equilibrium constants of affinity interactions between biological molecules.[2] The described mathematical tool enables new and valuable information to be extracted from existing analytical data published in close to 2000 scientific articles and from abundant unpublished data from the pharmaceutical industry.[3]

Affinity interactions are involved in regulation of practically all biological processes. Knowing molecular mechanisms that govern these interactions is of extreme importance to our understanding of normal cell function, disease, and drug action. At its basic level, the study of intermolecular interactions requires knowledge of their equilibrium constants and kinetics. For this purpose, binding molecules A and B with a formation of complex C can be described by a simple chemical equation:

$$\mathrm{C} \underset{k_+}{\overset{k_-}{\rightleftarrows}} \mathrm{A} + \mathrm{B} \qquad K_d = k_-/k_+ \tag{1}$$

where k_+ and k_- are rate constants of complex formation and dissociation, respectively, and K_d is the equilibrium dissociation constant. The goal of kinetic and thermodynamic studies is essentially to find k_+, k_-, and K_d.

A wide variety of methods is available that can only measure the K_d value; they can be called equilibrium methods.[4−8] This methodological variety accommodates the study of the vast diversity of biomolecular interactions, as each method offers different benefits and suffers from different limitations. Availability of robust methods for K_d measurement has made this parameter extremely important in pharmacology, where K_d values are often used as a primary screening criterion for candidate drug compounds. However, it is becoming more evident that knowledge of K_d is not sufficient for characterization of drug candidates, and that their interaction kinetics, characterized by k_+ and k_-, may play a far more important role.[9] This stems from the fact that biological processes rarely occur in equilibrium; thus, knowledge of interaction kinetics allows making more biologically relevant predictions. The current variety of kinetic methods is much more limited, with only surface plasmon resonance (SPR), biolayer interferometry (BLI), fluorescence correlation spectroscopy (FCS), and stopped-flow finding practical use.[10−12] SPR and BLI are surface-based methods, as they require immobilization of one of the interaction components, while FCS and stopped-flow are label-based, as they require labeling of at least one of the reaction components. Requirement for immobilization or labeling represents a major limitation of these methods, as

Received: December 1, 2013
Accepted: December 31, 2013
Published: December 31, 2013

   dx.doi.org/10.1021/ac4038976 | Anal. Chem. 2014, 86, 1298−1305

modification of components can influence the interaction between them by affecting their conformation or by introducing steric hindrance.[13,14] As a result, relatively few molecular biology studies or drug screening efforts take advantage of kinetic information. Development of solution-based label-free kinetic methods is, thus, highly desirable.

ACE was proposed as a solution-based label-free method for studying affinity interactions in the beginning of the 1990s.[15] Since its introduction, it has been acknowledged that ACE data contains equilibrium and kinetic information needed to find K_d, k_+, and k_-. However, extracting the convoluted k_+ and k_- necessitated the use of complicated numerical computation.[16] This likely explains the fact that throughout the two decades of existence, ACE has been used almost exclusively as a tool to find K_d values, and not k_+ and k_-. Nevertheless, ACE has found widespread application in analytical biochemistry and pharmaceutical research with thousands of papers published.[17]

In this article, we demonstrate that there exists an analytical solution of partial differential equations describing mass transfer in ACE. This analytical solution was developed by adapting mathematical equations from a related capillary electrophoresis (CE)-based method called Macroscopic Approach for Studying Kinetics at Equilibrium (MASKE).[18] The developed analytical solution allows accurate deconvolution of kinetic rate constants in a simple and rapid manner, without the need for specialized computer hardware, and can be easily implemented in any of the commonly available spreadsheet or computational software environments. The new mathematical tool expands applicability of ACE to a wider range of biomolecular interactions and allows prospective and retrospective determination of kinetic rate constants. This work shows how a "mathematical blade" can enable an old experimental tool to perform new challenging functions.

RESULTS AND DISCUSSION

Concepts of ACE and MASKE. In this section, we provide a conceptual description of ACE and discuss its similarity to MASKE, a related CE method. Conceptual similarities between the two methods suggest that mathematical tools developed for MASKE can be potentially used for analyzing ACE data.

ACE is an electrophoretic separation technique which is used study specific interactions between chemical or biological molecular species.[19] The experimental setup for ACE is conceptually depicted in Figure 1A, top row. In ACE, a capillary is prefilled with the run buffer that contains B. Species A is introduced into the capillary as a short plug, often as a part of an equilibrium mixture of A, B, and C (concentrations are denoted by the italicized letters: *A*, *B* and *C*). The total *B* (the sum of *B* and *C*) in the equilibrium plug is the same as *B* in the run buffer. The conditions are chosen so that the velocities of A and C in an electric field (v_A and v_C, respectively) differ. A and C are detected spectroscopically and their cumulative migration pattern is used to retrieve the information about reaction 1. It is important to indicate that equilibrium is not maintained in ACE experiments, as the formation of C causes localized depletion of B and, thus, variation of its concentration along the capillary. To avoid measurement errors caused by these concentration fluctuations, *B* is taken in excess of *A*.

Depending on how fast the equilibrium between A, B, and C is established, ACE electropherograms can present three general types of migration patterns corresponding to fast, slow, and intermediate equilibration. The assignment to one of the three cases is based on the relation between the

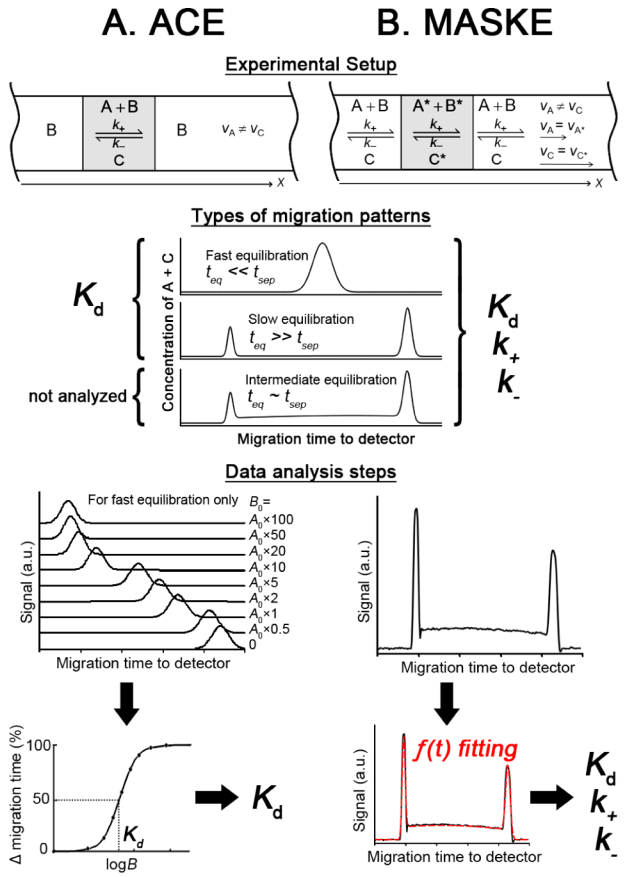

Figure 1. Conceptual similarities and differences between ACE (panel A) and MASKE (panel B). Top row: schematic representation of initial conditions; middle row: schematic representation of general types of migration patterns and the information that is extracted from each type; bottom row: schematic representation of steps in data analysis. See text for details.

characteristic equilibration time, t_{eq}, and the characteristic separation time, t_{sep}, which are defined as follows:

$$t_{eq} = 1/(k_+B + k_-), \quad t_{sep} = w/|v_A - v_C| \tag{2}$$

where w is the width of the initial zone of the equilibrium mixture. The cases of fast, slow, and intermediate equilibration correspond to $t_{eq} \ll t_{sep}$, $t_{eq} \gg t_{sep}$, and $t_{eq} \sim t_{sep}$, respectively. One can determine whether the equilibration is fast, slow, or intermediate without analyzing eqs 2, but by qualitatively analyzing the migration pattern of A and C. The three general cases of migration patterns are depicted in Figure 1, middle row. In the case of $t_{eq} \ll t_{sep}$, the equilibration between A and C in reaction 1 occurs much faster than separation of their respective zones, and, as a result, A and C will be moving as a single zone, producing a single peak in an ACE electropherogram. In the case of $t_{eq} \gg t_{sep}$, the zones of A and C will be separated before equilibration between them proceeds to a significant extent. Thus, A and C will be moving as separate zones, producing two separate peaks. In the case of $t_{eq} \sim t_{sep}$, equilibration and separation proceed with comparable rates; therefore, A and C will be moving as two zones with a significant overlap between them.

Historically, ACE was applied almost exclusively to cases with $t_{eq} \ll t_{sep}$. The velocity of the combined A and C zone is defined by a concentration-weighted average of v_A and v_C. Thus, gradual shifts in migration time of the combined peak

dx.doi.org/10.1021/ac4038976 | Anal. Chem. 2014, 86, 1298−1305

will occur as a function of B. These shifts in velocity of the single peak can be used as the single-parameter response for plotting of an isothermal binding curve, from which K_d can be determined graphically or though Scatchard analysis (Figure 1A, bottom row).[20] ACE data has been predominantly analyzed by this classic single-parameter approach for K_d determination. The k_+ and k_- constants, however, are convoluted within ACE electropherograms and are more difficult to extract. In 1993, Whitesides and coauthors reported on using a numerical computational approach to extract k_+ and k_- values from ACE data corresponding to the fast equilibration scenario.[16] This numerical approach, however, did not find any further application, most likely due to requirement of a considerable expertise in numerical computational methods and significant computing resources to produce accurate and stable solutions in a reasonable amount of time. More recently, Berezovski and colleagues developed a mathematical tool for approximation of k_+ and k_- from fast-equilibration ACE data by assuming rapid molecular exchange.[21] This tool, however, is only applicable to systems with large K_d values (between 8×10^{-5} and 3×10^{-3} mol L^{-1}) and very fast equilibration times (between 9×10^{-4} and 0.25 s), which limits its scope. Besides these two examples, ACE has not been used for determination of k_+ and k_-.

Systems that correspond to $t_{eq} \gg t_{sep}$ and $t_{eq} \sim t_{sep}$ are generally not analyzed by ACE. Determination of K_d for slow equilibrating systems is possible by analyzing pre-equilibrated sample mixtures and measuring the ratio between the areas of separate peaks of A and C; however, ACE is rarely used for study of such systems as simpler approaches, with no B in the run buffer, can be successfully used for this purpose.[22,23] Intermediate equilibration systems result in intricate migration patterns that have never been analyzed due to a lack of proper deconvolution tools.

Initial and boundary conditions in MASKE resemble those in ACE (Figure 1B, top row). To maintain chemical equilibrium, the entire capillary is filled with the equilibrium mixture of A, B, and C. In a short plug, however, A, and accordingly C, are labeled for detection (labeled components are denoted with an asterisk). While A+A*, B, and C+C* are in chemical equilibrium, the label creates informational nonequilibrium and allows one to follow the kinetics in reaction 1. Chemical equilibrium is maintained in MASKE, which has facilitated the development of an analytical solution for its partial differential equations of mass transfer of A* and C*.[18]

The relation between t_{eq} and t_{sep} play similar roles in MASKE and ACE. MASKE experiments that study interacting systems with fast, slow, and intermediate equilibration result in migration patterns similar to those of ACE (Figure 1, middle row). Unlike ACE, however, the analytical solution for MASKE allows k_+, k_-, and K_d to be extracted from all three types of migration patterns. One of the ways to achieve this is by fitting the available analytical solution for $A^* + C^*$ (t) into experimental migration patterns of the labeled components, while varying k_+ and k_-.

MASKE is a recently developed method that has not yet led to significant accumulation of data. The requirement of MASKE for labeling of A represents the same limitation as found in the other label-based kinetic methods: labeling may affect the interaction between A and B and may be difficult or expensive. This requirement also precludes the use of MASKE with the most popular label-free detection approach for CE–UV absorption spectroscopy. A simple and versatile experimental setup of ACE is generally preferable to that of MASKE.

The conceptual similarities between ACE and MASKE suggest that mathematical tools developed for MASKE may be adapted for analysis of ACE data. The ability to combine the simple experimental setup of ACE with the simple mathematical tools for MASKE would eliminate the limitations of each individual method. This study was motivated by the insight that the main difference between interaction conditions in ACE and MASKE lies in the concentration profile of B along the capillary: B is constant in MASKE, but not in ACE. However, if there is a sufficient excess of B over A, then the deviation of B from its nominal value becomes insignificant. Consistent with this notion, in silico simulated migration patterns of ACE and MASKE become more similar as B increases over A (Figure 2). Importantly, this condition is always satisfied in historical ACE experiments, as determination of K_d requires titration of B to achieve saturation in the formation of C.[20]

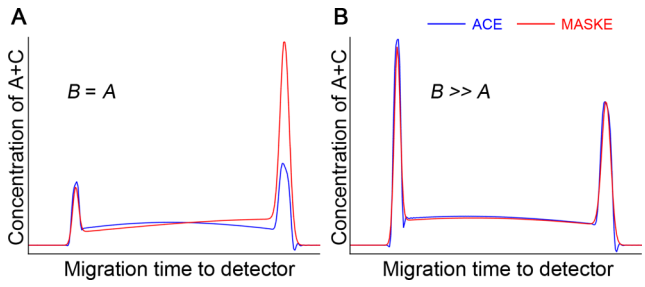

Figure 2. In silico simulated ACE (blue) and MASKE (red) migration profiles become more similar as total concentration of component B is increased over the concentration of component A. Panel A: A is equal to B; panel B: B is 10 times higher than A. ACE migration profile was simulated numerically, while MASKE migration profile was simulated using the available analytical solution. See text for simulation details. The profiles were simulated with the following values $k_+ = 3 \times 10^4$ M^{-1} s^{-1}, $k_- = 3 \times 10^{-3}$ s^{-1}, and $K_d = 100$ nM.

Similarity of Differential Equations and Their Solutions in ACE and MASKE. To determine if MASKE analytical solution can be adapted to ACE, we first show that differential equations of mass transfer that describe the two methods are identical if $B \gg \max(A, C)$. Diffusion is neglected throughout this consideration. The MASKE equations, which have been derived elsewhere,[18] are the following:

$$(\partial_t + v_A\partial_x)A^* = -k_+A^*B + k_-C^*$$
$$(\partial_t + v_C\partial_x)C^* = k_+A^*B - k_-C^* \quad (3)$$

where ∂_x and ∂_t are partial derivations by spatial coordinate and time, respectively. In MASKE, A^* and C^* change with time and coordinate, while B = const no regardless of the relation between B and A. In ACE, in general, the equation for B must also be considered so that the complete system involves three equations:

$$(\partial_t + v_A\partial_x)A = -k_+AB + k_-C$$
$$(\partial_t + v_B\partial_x)B = -k_+AB + k_-C$$
$$(\partial_t + v_C\partial_x)C = k_+AB - k_-C \quad (4)$$

where v_B is the velocity of B. Conditions at $t = 0$ for system 4 have the following form in the plug

$$A = A_{eq},\ B = B_{eq},\ C = C_{eq}\ (t = 0) \quad (5)$$

dx.doi.org/10.1021/ac4038976 | Anal. Chem. 2014, 86, 1298–1305

Here, A_{eq}, B_{eq}, and C_{eq} are equilibrium concentrations in the plug at $t = 0$. They can be calculated using equations

$$A_{eq} + C_{eq} = A_0,\ B_{eq} + C_{eq} = B_0,\ \frac{A_{eq}B_{eq}}{C_{eq}} = K_d \tag{6}$$

where A_0 and B_0 are concentrations of A and B used in the plug preparation (i.e., concentrations of A and B before formation of C).

By introducing dimensionless variables

$$\hat{A} = \frac{A}{A_0},\ \hat{B} = \frac{B}{B_0},\ \hat{C} = \frac{C}{A_0} \tag{7}$$

we can rewrite 4 as follows:

$$(\partial_t + v_A\partial_x)\hat{A} = -k_+B_0\hat{A}\hat{B} + k_-\hat{C}$$
$$(\partial_t + v_B\partial_x)\hat{B} = \lambda(-k_+B_0\hat{A}\hat{B} + k_-\hat{C})$$
$$(\partial_t + v_C\partial_x)\hat{C} = k_+B_0\hat{A}\hat{B} - k_-\hat{C} \tag{8}$$

Here $\lambda = A_0/B_0$ is a small parameter if B is taken in a sufficient excess to A during the plug preparation. In this case, a solution for eqs 6 can be obtained in a form of expansion in λ:

$$\hat{A} = \hat{A}_0 + \lambda\hat{A}_1 + ...$$
$$\hat{B} = \hat{B}_0 + \lambda\hat{B}_1 + ...$$
$$\hat{C} = \hat{C}_0 + \lambda\hat{C}_1 + ... \tag{9}$$

Substitution of 7 into the second equation in 6 and into conditions 5 and 6 yields

$$(\partial_t + \nu_B\partial_x)\hat{B}_0 = 0,\ \hat{B}_0 = 1(t = 0) \tag{10}$$

The first eq 10 has an obvious solution $\hat{B}_0(x,t) = \text{const}$. Given the second relation in eq 10, we finally have $\hat{B}(x,t) = \hat{B}_0 = 1$ in the zeroth order of approximation in λ. Substitution of $\hat{B} = 1$ in the first and last equations in 8 reduces the system of eqs 8 to two equations:

$$(\partial_t + v_A\partial_x)\hat{A} = -k_+B_0\hat{A} + k_-\hat{C}$$
$$(\partial_t + v_C\partial_x)\hat{C} = k_+B_0\hat{A} - k_-\hat{C} \tag{11}$$

After its transformation to the dimensional variables, system 11 is identical to MASKE eqs 3 (with $B = B_0$). Thus, differential equations for MASKE 3 and ACE 4 are identical (in the zeroth order of approximation in λ) when $B_0 \gg A_0$.

Since the differential equations for ACE 4 and MASKE 3 are approximately identical, their solutions will be similar if $\lambda \ll 1$ (with an error of the order of λ). The solution for MASKE eqs 3 is given elsewhere.[18] It was obtained by transition to the special dimensionless form of eqs 3 with subsequent application of Fourier transform in coordinate x. The resulting system of ordinary differential equations (in time t) was then solved for the following specific conditions at $t = 0$ (denoted by subscript 1 or 2)

$$A_1(x, 0) = \delta(x),\ C_1(x, 0) = 0 \tag{12}$$

$$A_2(x, 0) = 0,\ C_2(x, 0) = \delta(x) \tag{13}$$

where $\delta(x)$ is the Dirac delta function. These solutions have the following form:

$$A_1 = \left(\frac{|\omega|}{2}\sqrt{\frac{\eta}{\mu}}I_1(\rho) + \delta(\mu)\right)\gamma,\ C_1 = \frac{|\omega|\varepsilon}{2}I_0(\rho)\gamma,$$
$$A_2 = \frac{|\omega|}{2\varepsilon}I_0(\rho)\gamma,\ C_2 = \left(\frac{|\omega|}{2}\sqrt{\frac{\mu}{\eta}}I_1(\rho) + \delta(\eta)\right)\gamma \tag{14}$$

where

$$\varepsilon = \sqrt{k_+B/k_-},\ \omega = 2\sqrt{k_+k_-B}/(v_A - v_C)$$
$$\mu = v_At - x,\ \eta = x - v_Ct,\ \rho = |\omega|\sqrt{\mu\eta}$$
$$\varphi = \omega(\varepsilon - 1/\varepsilon)/2,\ \psi = \omega(v_C\varepsilon - v_A/\varepsilon)/2,\ \gamma = \exp(t\psi - x\varphi)$$

and I_0 and I_1 are modified Bessel functions of the first kind. Physical meaning of these parameters can be described as follows: ε^2 is a ratio of characteristic times of reverse and forward reactions 1; $1/\omega$ is a characteristic length describing the separation of A and C; relations $\mu = 0$ and $\eta = 0$ give motion laws for peaks of A and C; ρ is a dimensionless combination of coordinate x and time t that appears while solving 3; φ, ψ, and γ are some combinations that arise in transition to special dimensionless form of 3; γ partially describes the effect of reactions 1 on concentrations of A and C. Relations 14 are valid at $\mu\eta > 0$. In the opposite case, when $\mu\eta < 0$, the obtained analytical solution is a trivial one with $A_1 = C_1 = A_2 = C_2 = 0$. Strictly speaking, conditions 12 and 13 at $t = 0$ as well as solutions 14 correspond to the case when concentrations of A and C in the capillary are defined as linear concentrations (i.e., amounts of A and C per unit length). In this case, we can still use eqs 3 for linear concentrations A and C if B is defined as a volume concentration.

Solutions 14 represent two different types of Green functions for eqs 3 with conditions 12 or 13 defined at $t = 0$. For arbitrary distributions of volume concentrations $A^*(x,0)$ and $C^*(x,0)$ at at $t = 0$, the general solution of 3 can be easily expressed in terms of these Green functions:

$$A^*(x, t) = \int (A_1(x - y, t)A^*(y, 0) + A_2(x - y, t)C^*(y, 0))dy$$
$$C^*(x, t) = \int (C_1(x - y, t)A^*(y, 0) + C_2(x - y, t)C^*(y, 0))dy \tag{15}$$

Relations 15 combined with $B = B_0$ will also give (at $\lambda \ll 1$) an approximate solution for A and C in the case of ACE eqs 4, if we omit the asterisk on the left-hand side of expressions 15 and replace $A^*(y, 0)$ and $C^*(y, 0)$ with $A_{eq}(y)$ and $C_{eq}(y)$ on the right-hand side of expression 13. After this, the substitution of expressions 14 for A_1, C_1, A_2, and C_2 yields (at $v_C > v_A$):

$$A(x, t) = A_{eq}(x - v_At)\exp(-k_+Bt) +$$
$$\int_{x-v_Ct}^{x-v_At}\frac{|\omega|}{2}\sqrt{\frac{\eta_y}{\mu_y}}I_1(|\omega|\sqrt{\mu_y\eta_y})\exp(t\psi - (x - y)\varphi)A_{eq}(y)dy +$$
$$\int_{x-v_Ct}^{x-v_At}\frac{|\omega|}{2\varepsilon}I_0(|\omega|\sqrt{\mu_y\eta_y})\exp(t\psi - (x - y)\varphi)C_{eq}(y)dy \tag{16}$$

$$C(x, t) = C_{eq}(x - v_Ct)\exp(-k_-t) +$$
$$\int_{x-v_Ct}^{x-v_At}\frac{|\omega|\varepsilon}{2}I_0(|\omega|\sqrt{\mu_y\eta_y})\exp(t\psi - (x - y)\varphi)A_{eq}(y)dy +$$
$$\int_{x-v_Ct}^{x-v_At}\frac{|\omega|}{2}\sqrt{\frac{\mu_y}{\eta_y}}I_1(|\omega|\sqrt{\mu_y\eta_y})\exp(t\psi - (x - y)\varphi)C_{eq}(y)dy \tag{17}$$

dx.doi.org/10.1021/ac4038976 | Anal. Chem. 2014, 86, 1298−1305

where $\eta_y = x - y - v_C t$ and $\mu_y = v_A t - x + y$. In the case of $v_C < v_A$, integration in expressions 16 and 17 should be taken from $x - v_A t$ to $x - v_C t$.

It should be noted that all of the above equations use concentrations of A, B, and C, while in practice it might be more useful to operate with signal quantities of a given detection system (e.g., optical or electrochemical). It is instructive to consider the relations between the concentrations and signals using an example of fluorescence detection, although UV absorbance detection can be handled in the same way. If fluorescence detection is used, values A_{exp} and C_{exp} are related to measured fluorescence signals A_{fs} and C_{fs} as:

$$A_{exp} = \chi_A \frac{A_{fs}}{Q_A}, \quad C_{exp} = \chi_C \frac{C_{fs}}{Q_C} \tag{18}$$

where χ_A and χ_B are the proportionality coefficients, which depend on fluorophores and detectors used for A and C, and Q_A and Q_C are absolute quantum yields of A and C. In a typical case, a single fluorophore and a single detector are used for both A and C so that $\chi_A = \chi_B = \chi$. If we introduce a calibration coefficient $\alpha = \chi/Q_A$, then relations 16 can be presented in a more practical form:

$$A_{exp} = aA_{fs}, \quad C_{exp} = \alpha \frac{C_{fs}}{\beta} \tag{19}$$

where $\beta = Q_C/Q_A$ is a relative quantum yield, which is measured much easier than absolute quantum yields.

Finding k_+ and k_-. Relations 16 and 17 can be used to find k_+ and k_- from experimental ACE data in a "pattern-based approach".[24] To do this, one should use nonlinear regression in which migration patterns of *A* and *C*, calculated with 16 and 17, are used to fit experimentally obtained A_{exp} and C_{exp} at various sets of k_+ and k_- and fixed known values of initial concentrations and migration velocities. The best fit will give values of k_+ and k_-. If A and C are indistinguishable in detection (e.g., spectrally), then the sum of $A + C$ should be calculated from 16 and 17 and fitted into the experimentally obtained sum of $A_{exp} + C_{exp}$. Pattern-based approaches for finding k_+ and k_- in ACE are technically similar to those used in SPR or stopped-flow kinetic methods.

Alternatively, simple multiparameter-based approaches for approximating k_+ and k_- in MASKE have been developed and are described elsewhere.[18,25,26] Such approaches are equally applicable to ACE. They rely on certain simplifying assumptions that, in turn, allow finding algebraic equations for k_+ and k_-. The equations include several parameters such as migrations times, peak widths, peak heights, and peak areas. Different assumptions are made for slow, fast, and intermediate equilibration.

Dependence of ACE Kinetic Measurement Accuracy on Initial Conditions. The mathematical tools described in the previous section can be used to extract k_+ and k_- from ACE electropherograms, as long as the chosen initial concentration of B is sufficiently higher than that of A. From the practical standpoint, it would be useful to know how the accuracy of ACE kinetic measurement changes with varying ratios of these concentrations. To allow the end-users to determine suitable conditions for data analysis, we have performed an in silico study of ACE kinetic measurement accuracy for different equilibration−time scenarios and over a wide range of component concentrations.

To simulate ACE migration patterns, we have employed a numerical computational approach, similar to the previously described.[16] We used COMSOL Multiphysics environment, version 4.3a, with the "Transport of Diluted Species" module, which incorporates mass balance equations, chemical reactions, convective and electrophoretic terms, and Fick's law of diffusion to approximate migration patterns of defined species within discrete-space geometry. Direct MUMPS solver was used to approximate concentrations of molecules A and B, and their complex C, in a time-dependent manner over a defined 1D geometry that modeled a capillary. One hundred and seventy ACE migration patterns, with different combinations of k_+ and k_-, as well as values of A_0 and B_0, were generated. Analytical eqs 16 and 17 were programmed into COMSOL Multiphysics variable set, and the "Optimization" module was used to back-calculate the k_+ and k_- values analytically, with numerically simulated curves set as the global least-squares objectives. Direct PARADISO solver, using the Levenberg−Marquardt optimization method was used to determine k_+ and k_- values that produced the best fit. Relative errors between the input and the back-calculated k_+ and k_- values for systems with different characteristic equilibration times appear in Figure 3. To ensure the highest sensitivity of measurement, B_0 was chosen to be equal to the K_d value, while A_0 was lowered to achieve various B_0/A_0 values. As expected, the largest error in

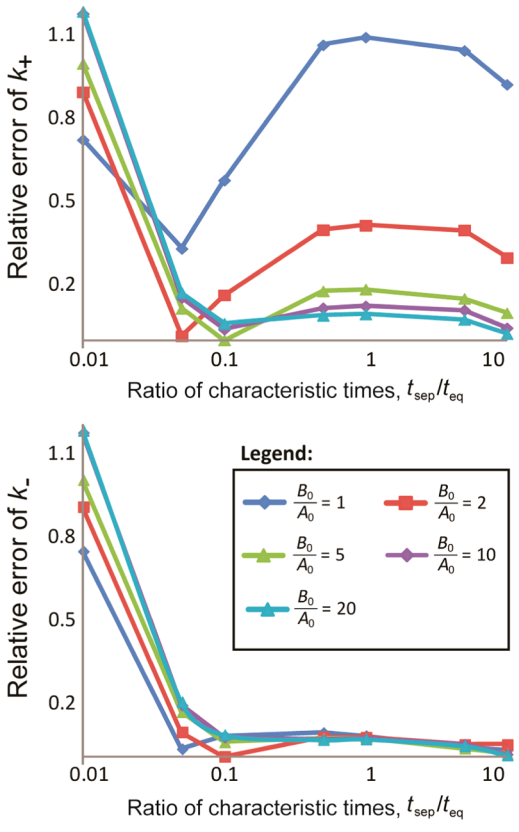

Figure 3. Accuracy of ACE kinetic measurements at various B_0 and A_0. Top and bottom panels show relative errors of k_+ and k_-, respectively. The errors are defined as ratios between input and back-calculated values of the rate constants. Measurement errors were evaluated for interacting systems with characteristic equilibration times ranging from slow ($t_{sep}/t_{eq} = 0.01$) to fast ($t_{sep}/t_{eq} = 10$) scenarios. For all traces, B_0 was chosen to equal K_d, while A_0 was lowered to achieve varying values of B_0/A_0 (see the legend in the figure).

dx.doi.org/10.1021/ac4038976 | Anal. Chem. 2014, 86, 1298−1305

determination of k_+ was observed when $B_0 = A_0$, with relative error exceeding 1 for systems with fast characteristic equilibration times. The errors reduced significantly when the B_0/A_0 ratio was increased to 2 and 5, while further increases to 10 and 20 produced less significant improvements. Regardless of the ratios of concentrations used in the simulations, measurements in systems that had a very slow characteristic equilibration time ($t_{sep}/t_{eq} < 0.01$) produced high errors. This is due to the fact that in such systems few association and dissociation events occur during separation, thus resulting in migration patterns that contain little information on interaction kinetics. In contrast, small errors were observed in measurements of systems with moderately slow ($t_{sep}/t_{eq} \sim 0.1$) and intermediate ($t_{sep}/t_{eq} \sim 1$) equilibration times. This stems from the fact that such migration patterns (two peaks and a connecting bridge region) contain the most features that the curve-fitting software can use to extract unknown parameters. Simulated electropherogram peaks that resulted from analysis of systems with very fast equilibration times ($t_{sep}/t_{eq} > 10$) had shapes which were indistinguishable from the shape of the initial sample plug analyte distribution. As a result, kinetic constants could not be extracted from data obtained for such cases. Accuracy of k_- determination did not change significantly with A_0/B_0 ratios, as dissociation rates do not depend on B. Similar trends were observed when B_0 was different from the value of K_d, albeit with larger errors (Figure S1). These results suggest that a 5-fold excess of B_0 over A_0 is sufficient to conduct kinetic analysis of ACE data with relative errors under 20%.

Retrospective Analysis of Historical ACE Data. To demonstrate the power of the new approach in retrospective analysis of ACE data, we applied it to two different historical studies. The first study is the prominent work by Whitesides and coauthors,[16] where a numerical approach was applied for the first time to extract k_+ and k_- values from ACE data. Using this data has enabled us to compare and validate our results against the values produced by the original study. This study investigated the affinity interaction between bovine carbonic anhydrase (CA) and a charged arylsulfonamide ligand (ASL). In this experiment, CA and ASL correspond to molecules A and B, respectively.

To calculate the ACE migration patterns using our analytical solution, the following information was obtained from the "Materials and Methods" section of the original article: initial concentrations of CA and ASL, applied voltage, total and effective lengths of the capillary, and the length of the initial sample plug. Concentration-to-signal conversion multipliers and electrophoretic mobilities of free CA and CA–ASL complex were approximated from experimental data. Electrophoretic mobility of free ALS was approximated to be 50% slower than that of CA–ASL complex: precise knowledge of this value is not required, as electrophoretic mobility of B does not have a significant effect on migration patterns of systems that undergo fast equilibration ($t_{eq} \ll t_{sep}$). The experimental electropherograms were digitized from the original publication using open-source Engauge Digitizer software, version 4.1. Equations 16 and 17 were programmed into COMSOL Multiphysics variable set, and the "Optimization" module was used in the same way as described in the previous section, except the digitized experimental curves were used as the global least-squares objectives. In the original experiments, CA was maintained at a concentration of 1×10^{-5} mol L^{-1}, while ASL was titrated between 0 and 2×10^{-4} mol L^{-1}. Only the electropherograms with $B_0/A_0 \geq 5$ were used for fitting aiming at accurate determination of k_+ and k_- (Figure 4A). The obtained values, $k_+ = (4.36 \pm 0.09) \times 10^4$ L mol^{-1} s^{-1},

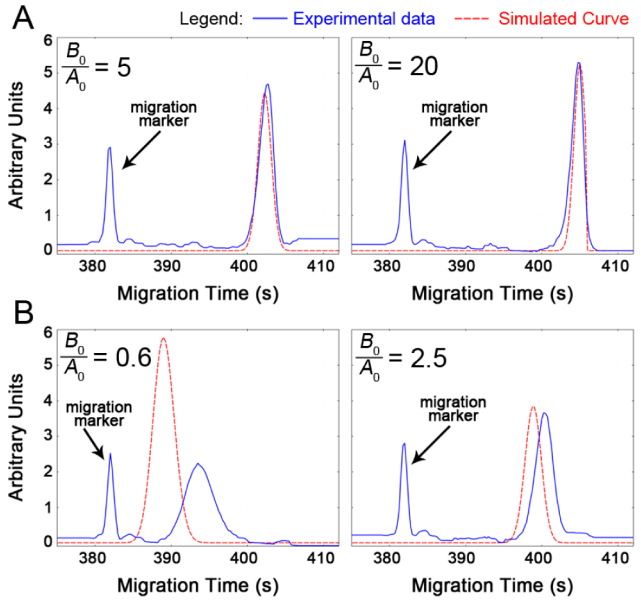

Figure 4. Experimental and simulated ACE migration patterns describing interaction between CA (molecule A) and ASL (molecule B). Panel A: k_+, k_- and K_d were determined by fitting the historical data in which $B_0/A_0 \geq 5$. Panel B: curves simulated with the obtained parameters poorly matched the experimental data when $B_0/A_0 \ll 5$, but improved as the ratio approached 5. The peak on the left is a noninteracting migration marker, and it was not included in the fitting.

$k_- = 0.31 \pm 0.08$ s^{-1}, and $K_d = (7.03 \pm 0.03) \times 10^{-6}$ mol L^{-1}, closely matched the values reported in the original publication, $k_+ = 1.5 \times 10^4$ L mol^{-1} s^{-1}, $k_- = 0.1$ s^{-1}, and $K_d = 7 \times 10^{-6}$ mol L^{-1}. The errors reported with our values represent the precision of fitting different experimental traces, and they are indicative of the high quality of the original experimental data. It should be noted that according to our in silico study, described in the previous section, a systematic error of 10–20% might be affecting our results, potentially explaining the difference between our values compared to those reported in the original study. Furthermore, this difference may also be explained by the fact that the original study only considered only three possible combinations of k_+ (1.5×10^5, 1.5×10^4, and 1.5×10^3 L mol^{-1} s^{-1}) and k_- (1, 0.1, and 0.01 s^{-1}) values in their simulations, most likely due to the long time requirements of numerical computation. Our analytical solution allowed us to simulate hundreds of possible k_+ and k_- combinations within a few minutes, likely yielding more refined values. As predicted by our in silico study, the electropherograms simulated with the obtained k_+ and k_- values did not produce a satisfactory fit with the experimental data when B_0/A_0 was significantly below 5, but the fit improved as the value approached 5 (Figure 4B). These findings strongly support the validity of the new mathematical approach.

Lastly, the new mathematical tool was applied for retrospective analysis of a recent study by Liu and colleagues.[27] This work simultaneously investigated the affinity interaction between three boronic acids (molecules A) and fructose (molecule B). The boronic acids under investigation were phenylboronic acid (PB), 3-carboxyphenylboronic acid (CP), and 3-carboxybenzoboroxole (CB). Experimental conditions

dx.doi.org/10.1021/ac4038976 | Anal. Chem. 2014, 86, 1298–1305

and experimental traces were retrieved from the original publication and analyzed as described in the first example. The following values were obtained by fitting: for PB $k_+ = 176 \pm 19$ L mol^{-1} s^{-1}, $k_- = 1.10 \pm 0.01$ s^{-1}, $K_d = (6.3 \pm 0.7) \times 10^{-3}$ mol L^{-1}; for CP $k_+ = 19.5 \pm 9.7$ L mol^{-1} s^{-1}, $k_- = 0.11 \pm 0.04$ s^{-1}, $K_d = (6.1 \pm 2.7) \times 10^{-3}$ mol L^{-1}; and for CB $k_+ = 179 \pm 108$ L mol^{-1} s^{-1}, $k_- = 0.6 \pm 0.3$ s^{-1}, $K_d = (4.0 \pm 0.9) \times 10^{-3}$ mol L^{-1} (Figure 5). To the best of our knowledge, this is the first instance when kinetics of interaction for these molecular pairs have been reported. This example clearly demonstrates the power and capacity of the new approach to produce new and valuable information from existing data. We anticipate that the new mathematical tool will find a wide use in both the analytical and pharmacological communities that employ, or have employed, ACE.

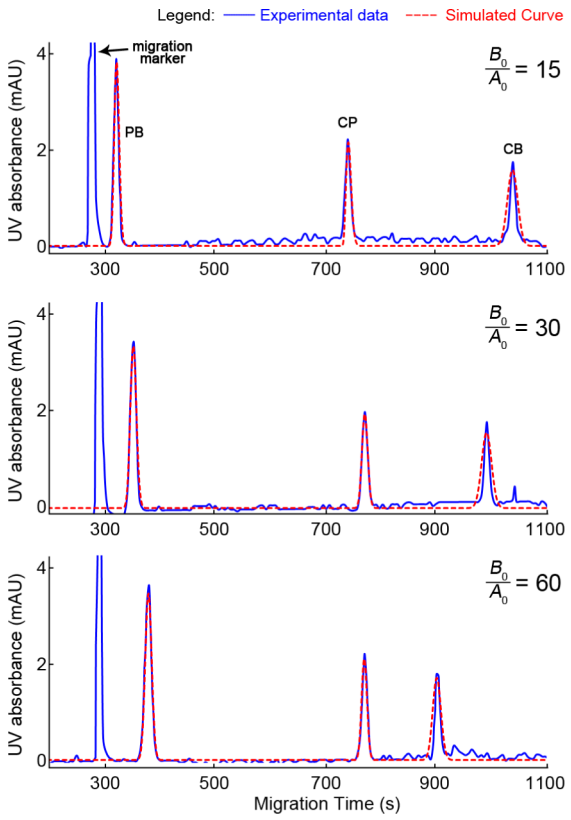

Figure 5. Experimental and simulated ACE migration patterns describing interaction between PB, CP, and CB (molecules A) and fructose (molecule B). From top to bottom: determination of k_+, k_- and K_d by fitting historical data in which B_0/A_0 were equal to 15, 30, and 60. The peak on the left is a noninteracting migration marker and was not included in the fitting. The peak for each boronic acid species was fitted individually, but then it was combined into a single curve, containing all three peaks for convenient representation.

CONCLUDING REMARKS

We proved theoretically and confirmed through retrospective analysis of previously published data that the propagation patterns of A and C in ACE and A* and C* in MASKE are identical if $B_0 \gg A_0$. Choosing B_0 that is at least 5-fold higher than A_0 will satisfy this condition for majority of interaction systems. This allows one to apply general solution 12 to ACE electropherograms. This also enables the use of the simplified approximate methods for finding rate constants from ACE data. Kinetic measurements by ACE become especially useful when labeling of component A is undesirable. Given the fact that in ACE the component B is always taken in excess to component A, the new mathematical tool can be used retrospectively to extract kinetic information from all historical ACE experiments for which the original electropherograms are available.

ASSOCIATED CONTENT

Supporting Information

Additional information as noted in the text. This material is available free of charge via the Internet at http://pubs.acs.org.

AUTHOR INFORMATION

Corresponding Author

*E-mail: skrylov@yorku.ca.

Notes

The authors declare no competing financial interests.

ACKNOWLEDGMENTS

This work was funded by the Natural Sciences and Engineering Research Council of Canada. M.K. was supported by the Alexander Graham Bell Canada Graduate Scholarship.

REFERENCES

(1) Zhao, S.; Fernald, R. D. *J. Comput. Biol.* **2005**, *12*, 1047−1064.
(2) Chu, Y. H.; Avila, L. Z.; Gao, J. M.; Whitesides, G. M. *Acc. Chem. Res.* **1995**, *28*, 461−468.
(3) Neubert, R. H. H.; Schwarz, M. A.; Mrestani, Y.; Platzer, M.; Raith, K. *Pharm. Res.* **1999**, *16*, 1663−1673.
(4) Hellman, L. M.; Fried, M. G. *Nat. Protoc.* **2007**, *2*, 1849−1861.
(5) Leavitt, S.; Freire, E. *Curr. Opin. Struct. Biol.* **2001**, *11*, 560−566.
(6) Chen, H. M.; Puhl, H. L.; Ikeda, S. R. *J. Biomed. Opt.* **2007**, *12*, 9.
(7) Ozers, M. S.; Hill, J. J.; Ervin, K.; Wood, J. R.; Nardulli, A. M.; Royer, C. A.; Gorski, J. *J. Biol. Chem.* **1997**, *272*, 30405−30411.
(8) Wienken, C. J.; Baaske, P.; Rothbauer, U.; Braun, D.; Duhr, S. *Nat. Commun.* **2010**, *1*, 7.
(9) Copeland, R. A. *Expert Opin. Drug Discovery* **2010**, *5*, 305−310.
(10) Schuck, P. *Annu. Rev. Biophys. Biomol. Struct.* **1997**, *26*, 541−566.
(11) Olson, S. T.; Srinivasan, K. R.; Bjork, I.; Shore, J. D. *J. Biol. Chem.* **1981**, *256*, 1073−1079.
(12) Schwille, P.; Haupts, U.; Maiti, S.; Webb, W. W. *Biophys. J.* **1999**, *77*, 2251−2265.
(13) Osmond, R. I. W.; Kett, W. C.; Skett, S. E.; Coombe, D. R. *Anal. Biochem.* **2002**, *310*, 199−207.
(14) Secundo, F. *Chem. Soc. Rev.* **2013**, *42*, 6250−6261.
(15) Chu, Y. H.; Avila, L. Z.; Biebuyck, H. A.; Whitesides, G. M. *J. Med. Chem.* **1992**, *35*, 2915−2917.
(16) Avila, L. Z.; Chu, Y. H.; Blossey, E. C.; Whitesides, G. M. *J. Med. Chem.* **1993**, *36*, 126−133.
(17) Heegaard, N. H. H.; Kennedy, R. T. *Electrophoresis* **1999**, *20*, 3122−3133.
(18) Krylov, S. N.; Okhonin, V.; Berezovski, M. V. *J. Am. Chem. Soc.* **2010**, *132*, 7062−7068.
(19) Riekkola, M. L.; Jonsson, J. A.; Smith, R. M. *Pure Appl. Chem.* **2004**, *76*, 443−451.
(20) Colton, I. J.; Carbeck, J. D.; Rao, J.; Whitesides, G. M. *Electrophoresis* **1998**, *19*, 367−382.
(21) Mironov, G. G.; Okhonin, V.; Gorelsky, S. I.; Berezovski, M. V. *Anal. Chem.* **2011**, *83*, 2364−2370.
(22) Heegaard, N. H. H.; Nilsson, S.; Guzman, N. A. *J. Chromatogr. B* **1998**, *715*, 29−54.
(23) Jiang, C. X.; Armstrong, D. W. *Electrophoresis* **2010**, *31*, 17−27.
(24) Petrov, A.; Okhonin, V.; Berezovski, M.; Krylov, S. N. *J. Am. Chem. Soc.* **2005**, *127*, 17104−17110.
(25) Cherney, L. T.; Krylov, S. N. *Anal. Chem.* **2011**, *83*, 1381−1387.

(26) Cherney, L. T.; Krylov, S. N. *Anal. Chem.* **2012**, *137*, 1649−1655.
(27) Lu, C. C.; Li, H. Y.; Wang, H. Y.; Liu, Z. *Anal. Chem.* **2013**, *85*, 2361−2369.